Available online at www.sciencedirect.com
ScienceDirect
International Journal of Thermal Sciences 47 (2008) 1113–1122
International Journal of Thermal Sciences
www.elsevier.com/locate/ijts

Study of heat transfer augmentation in a differentially heated square cavity using copper–water nanofluid

Apurba Kumar Santra [a,*], Swarnendu Sen [b], Niladri Chakraborty [a]

[a] *Department of Power Engineering, Jadavpur University, Salt Lake Campus, Block – LB, Plot-8, Sector – III, Salt Lake, Kolkata 700 098, India*
[b] *Department of Mechanical Engineering, Jadavpur University, Kolkata 700 032, India*

Received 26 September 2006; received in revised form 11 September 2007; accepted 17 October 2007

Available online 3 December 2007

Abstract

Effect of copper–water nanofluid as a cooling medium has been studied to simulate the behavior of heat transfer due to laminar natural convection in a differentially heated square cavity. The transport equations for a non-Newtonian fluid have been solved numerically following finite volume approach using SIMPLER algorithm. The shear stresses have calculated using Ostwald–de Waele model for an incompressible non-Newtonian fluid. The thermal conductivity of the nanofluid has been calculated from the proposed model by Patel et al. Study has been conducted for Rayleigh number (Ra) 10^4 to 10^7 while solid volume fraction (ϕ) of copper particles in water varied from 0.05% to 5%. It has been observed that the heat transfer decreases with increase in ϕ for a particular Ra, while it increases with Ra for a particular ϕ. The copper nanoparticle diameter has been taken as 100 nm for all of the studies.

Keywords: Nanofluid; Heat transfer; Non-Newtonian; Natural convection; Square cavity

1. Introduction

A suspension of solid nanoparticles (1–100 nm diameter) in conventional liquids like water, oil or ethylene glycol (EG) is called nanofluid. Since thermal conductivity of these base liquids are low, enhancing performance (reliability and life) of many engineering devices are becoming a problem. Several researches [1–3] have indicated that with low (1–5% by volume) nanoparticle concentration, the thermal conductivity can be increased by about 20%. Such enhancement depends on shape, size, concentration and thermal properties of the solid nanoparticles. Sometimes stabilizer is added with the nanofluid to stabilize the solid particles in the mixture [4]. The nanofluid is stable [5], introduce very little pressure drop and it can pass through nano-channels. Xuan et al. [3] experimentally obtained thermal conductivity of copper–water nanofluid up to 7.5% of solid volume fraction of 100 nm diameter copper particles. They have also observed that this nanofluid with 5% solid volume fraction remains stable for more than 30 hours without disturbance.

Since nanofluid behaves like a fluid than a mixture, several researchers have tried to explain the physics behind the increase in thermal conductivity. Xuan et al. [6] have examined the transport properties of nanofluid and the thermal dispersion effect with two different approaches, the conventional approach and the modified approach. In the conventional approach the existing heat transfer coefficient correlations for the pure fluid are directly extended to the nanofluid, substituting the thermal properties of nanofluid for those of pure fluid. In the modified approach the thermal dispersion, which takes place due to the random movement of particles, has been considered. This thermal dispersion will flatten the temperature distribution and make the temperature gradient between the fluid and wall steeper, increasing the heat transfer rate between the fluid and the wall [6]. So far as no theoretical or experimental study has been published on the constants that will correlate the thermal diffusivity and thermal dispersion. Keblinski et al. [7] has expressed that heat transfer enhancement in nanofluid can also be affected by the Brownian motion of the particles, molecular

* Corresponding author. Tel.: +91 33 2335 5813/5215; fax: +91 33 2335 7254.
E-mail address: aksantra@pe.jusl.ac.in (A.K. Santra).

1290-0729/$ – see front matter
doi:10.1016/j.ijthermalsci.2007.10.005

Nomenclature

c	specific heat	J/kg K	
Gr_f	Grashof number of fluid, $\rho^2 g\beta\Delta T H^3/\mu^2$		
g	acceleration due to gravity	m/s^2	
h, l	dimensional height and width of cavity	m	
k	thermal conductivity	W/mK	
m, n	the respective consistency and fluid behaviour index parameters		
Nu_y	local Nusselt number of the heater		
$\overline{Nu}$	average Nusselt number of the heater		
p	pressure	N/m^2	
P	dimensionless pressure, $(p-p_0)h^2/\rho_0\alpha^2$		
Pr	Prandtl number of fluid, ν_f/α_f		
Ra	Raleygh number, $Gr\,Pr$		
T	temperature	K	
T_H, T_C	temperature of the heat source and sink respectively	K	
u, v	velocity components in the x and y directions respectively	m/s	
U, V	dimensionless velocities ($U = uh/\alpha$, $V = vh/\alpha$)		
x, y	horizontal and vertical coordinates respectively	m	
X, Y	dimensionless horizontal and vertical coordinates respectively ($X = x/h$, $Y = y/h$)		

Greek symbols

α	thermal diffusivity of the fluid	m^2/s
β	isobaric expansion coefficient	K^{-1}
ϕ	solid volume fraction	
μ	dynamic viscosity	$N\,s/m^2$
ν	kinematic viscosity	m^2/s
ρ	density of the fluid	kg/m^3
θ	dimensionless temperature, $(T-T_0)/(T_H-T_C)$	
ψ	dimensionless stream function	
τ	the stress tensor	
$\dot{\gamma}$	the symmetric rate of deformation tensor	

Subscripts

eff	effective
f	fluid
nf	nanofluid
0	at reference state
s	solid

level layering of liquid at the liquid/particle interface, ballistic phonon transport through the particles and nanoparticle clustering. It has been shown that the heat transport in nanofluid is ballistic rather than diffusive and particle-clustering effect takes a major role for rapid heat transport through nanofluids. Later the same group has shown by molecular dynamic simulation that large enhancement in thermal conductivity of nanofluid cannot be explained by altered thermal transport properties of the nanofluid [8]. Das et al. [9] has observed that the thermal conductivity for nanofluid increases with increasing temperature. They have also observed the stability of Al_2O_3–water and CuO–water nanofluid. Even up to 12 hours no sedimentation was observed keeping those undisturbed [9]. The stability can be increased by adding suitable third agent like oleic acid or laurate salt [3,9].

Due to lack of sophisticated theory to predict the effective thermal conductivity of nanofluid several researchers have proposed different correlations to predict the apparent thermal conductivity of two-phase mixture. The models proposed by Hamilton and Crosser (HC) [10], Wasp [11], Maxwell-Garnett [12], Bruggeman [13] and Wang et al. [14] to determine the effective thermal conductivity of nanofluid failed to predict it accurately. The experimental results show a much higher thermal conductivity of nanofluid than those predicted by these models. Yu and Choi [15] has proposed a renovated Maxwell model considering the liquid layer thickness which is proved to be not realistic [8] and it fails to throw light on the temperature dependence of thermal conductivity. Kumar et al. [16] has proposed a model that has two aspects. A stationary particle model, where it is assumed that heat flows through two paths, one through liquid particles and other through nanoparticles. In the moving particle model, along with the above, the increase in effective thermal conductivity of nanofluid due to increase in velocities of the nanoparticles with temperature has been taken into account. In both cases the thermal conductivity decreases with the increase in particle diameter. Recently Prasher et al. [17] have showed that the enhancement of k_{eff} of nanofluid is mainly due to the localized Brownian movement of nanoparticles. They have also proposed a conduction–convection based model to find the k_{eff} of nanofluid. They have contradicted model of Ref. [16] because their model does not remain valid when particle radius is very large and they have assumed mean free path as 1 cm. But the model of Ref. [16] is valid for nanofluid (particle diameter in the order of nm) and the empirical correlation has a constant, which is adjustable [18,19]. Patel et al. [20] has improved the model given in [16] by incorporating the effect of micro-convection due to particle movement. The effect of temperature is justified as Brownian motion increases with temperature, which causes additional convective effect. The above model is applicable for low concentration of solid volume fraction. Also the model takes into account the effect of particle size through an increase in specific surface are of nanoparticles [18]. There involves an empirical constant 'c', to link the temperature dependence of effective thermal conductivity to the Brownian motion of the particles. This can be found by comparing the calculated value with experimental data, which comes in the order of 10^4. This empirical constant 'c' is adjustable and can be thought as a function of particle properties as well as size [20].

Xuan and Li [21] have investigated the convective heat transfer and flow features of nanofluid in a tube. For turbulent flow they have correlated the Nusselt number as a function of ϕ, Peclet number (Pe), Reynolds number (Re) and Prandtl number (Pr). They presumed that the Pe describes the effect of thermal

dispersion. Later Yang et al. [22] have studied experimentally the convective heat transfer of nanofluid for laminar flow in a horizontal tube heat exchanger. Recently Boungiorno [23] has shown analytically that thermal dispersion has a negligible effect on such increase in convective heat transfer rather Brownian diffusion and thermo-phoresis are the main mechanism that contributes to the heat transfer enhancement. However Koo et al. [24] have shown that the Brownian motion has more impact on the thermal properties of nanofluid than thermo-phoresis. Heris et al. [25] has experimentally investigated laminar flow forced convection heat transfer of Al_2O_3–water nanofluid in a circular tube with constant wall temperature. They have used the renovated Maxwell model [15] to determine the thermal conductivity of the nanofluid with a liquid layer thickness of 10% of the nanoparticle radius. They have reported that the heat transfer co-efficient increases due to presence of nanoparticles. Heris et al. [26] have carried experiment with Al_2O_3–water and CuO–water nanofluid up to $\phi = 3\%$ and have shown that up to this limit the nanofluid behaves like Newtonian fluid.

Several researchers have tried to reveal the rheology of nanofluid. They have shown that the well-known viscosity model given by Brinkman [27] is not applicable for nanofluid. Kwak and Kim [28] have experimentally observed the viscosity of CuO–EG nanofluid. They have found that the viscosities of nanofluid depend on shear thinning and zero shear viscosity increases rapidly when ϕ exceeds 0.2%. Chang et al. [29] also found experimentally that CuO–water nanofluid shows shear thinning behaviour and shear stress increases with particle size for a particular shear rate. Also they have shown that viscosity of nanofluid increases with decrease in mean particle size. Ding et al. [30] experimentally measured the viscosity of CNT–water nanofluid under various conditions and observed a clear shear thinning behaviour at all conditions. They have also observed that for a given shear rate, the viscosity of nanofluid increases with increasing concentration and decreasing temperature. Maiga et al. [31] have given a correlation of viscosity of γAl_2O_3–water nanofluid with ϕ which shows that the effective viscosity is much more than predicted by Brinkman model [27].

Though an extensive research work has been carried out on natural convection, very few literatures are found regarding natural convection heat transfer using nanofluid. Natural convection in suspensions with micrometer-sized particles has been studied by Okada and Suzuki [32] with microbeads of soda glass in water and Kang et al. [33] with SiO_2 particles in water. Putra et al. [34] has experimentally observed the effect of Al_2O_3–water and CuO–water nanofluid on Nusselt number (Nu) for different Rayleigh number (Ra) due to natural convection in a differentially heated horizontal cylinder. Their observation was contrary to their expectations, as with the increase in particle concentration the Nu decreases which could not be explained. They have also shown that viscosity of nanofluid increases with ϕ and also measured the shear stress for different shear rate of Al_2O_3–water nanofluid for different ϕ. Recently Wen and Ding [35] have experimentally observed the natural convective heat transfer in a differentially heated vertical cylinder heated from the bottom with TiO_2–water nanofluid. Their observation is almost similar to that of [34], where the convective heat transfer co-efficient decreases with that of increase of nanoparticles. They have also shown that viscosity of this nanofluid increases rapidly with inclusion of nanoparticles as shear rate decreases.

Khanafer et al. [36] have performed a numerical study of heat transfer enhancement following Wasp model [11] using copper nanofluid in a square cavity. They have considered the thermal dispersion but that involves an empirical constant, which is still unknown. Jou et al. [37] have performed same study as of [36] to observe the effect of aspect ratio of the enclosure on heat transfer for Cu–water nanofluid considering ϕ up to 20%. Santra et al. [38] have conducted the similar kind of study, up to $\phi = 10\%$, with models given in [12] and [13]. This shows that the Brugemann model [13] predicts higher heat transfer than Maxwell-Garnett model [12]. They have not considered the thermal dispersion. In all of the above studies the nanofluid has been considered as Newtonian.

The study on nanofluid is promising for nanotechnology based cooling applications such as MEMS, including ultrahigh thermal conductivity coolants, lubricants, hydraulic fluids and metal cutting fluids. Since, under off normal condition the natural convection is the only mode of heat transfer, the components may be more prone to damage.

The present paper shows the effect copper–water nanofluid on the heat transfer due to natural convection in a differentially heated square cavity treating the nanofluid as non-Newtonian in nature. To determine the effective thermal conductivity (k_{eff}) of the nanofluid, model given by Patel et al. [20] has been used with appropriate value of 'c', which has been calculated by matching the experimental result. Since no other model takes care of the temperature dependence of k_{eff}, this model has been considered as best option. The viscosity of nanofluid has been calculated using Ostwald–de Waele model (two parameter power law model) for a non-Newtonian shear thinning fluid [39]. To the best of the knowledge of the authors, no other numerical study on buoyancy driven heat transfer analysis using nanofluid particularly considering the fluid as non-Newtonian and the aforesaid thermal conductivity model has been reported so far. Here the authors have used the primitive variables, instead of stream function and vorticity method [36,37].

2. Mathematical formulation

2.1. Problem statement

The geometry of the present problem is shown in Fig. 1. It consists of a two-dimensional square enclosure of height h and width l. For the present case, we consider $h = l$. The temperatures of the two sidewalls of the cavity are maintained at T_H and T_C, where T_C has been considered as the reference condition. The top and the bottom horizontal walls have been considered to be insulated i.e., non-conducting and impermeable to mass transfer. The enclosure is filled with a mixture of water and solid spherical copper particles of 100 nm diameter. The nanoparticles are of uniform shape and size. The nanofluid is assumed to be non-Newtonian, incompressible and the flow is laminar. Also it is assumed that the liquid and solid are in

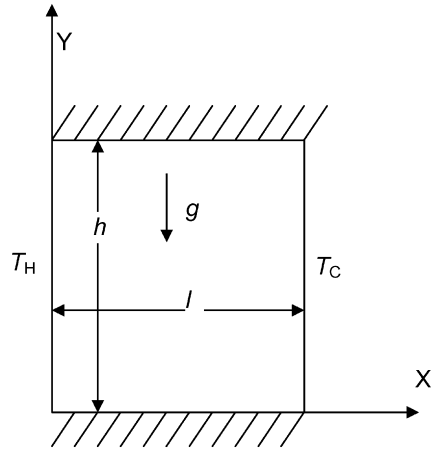

Fig. 1. Geometry of the problem.

thermal equilibrium and they flow at same velocity. The density varies only in buoyant force, which has been incorporated only in the body force term by employing the Boussinesq approximation. For all the studies $h = l$ has been considered.

2.2. Governing equations and boundary conditions

The continuity, momentum and energy equations for a steady, two-dimensional flow of a Fourier constant property fluid have been considered. The governing equations for a steady, two-dimensional flow are as follows

$$\frac{\partial u}{\partial x} + \frac{\partial v}{\partial y} = 0 \tag{1}$$

$$\rho_{\mathrm{nf},0}\left(u\frac{\partial u}{\partial x} + v\frac{\partial u}{\partial y}\right) = -\frac{\partial p}{\partial x} - \left[\frac{\partial \tau_{xx}}{\partial x} + \frac{\partial \tau_{yx}}{\partial y}\right] \tag{2}$$

$$\rho_{\mathrm{nf},0}\left(u\frac{\partial v}{\partial x} + v\frac{\partial v}{\partial y}\right) = -\frac{\partial p}{\partial y} + \left[\phi\rho_{s,0}\beta_s + (1-\phi)\rho_{f,0}\beta_f\right]g(T - T_C) - \left[\frac{\partial \tau_{xy}}{\partial x} + \frac{\partial \tau_{yy}}{\partial y}\right] \tag{3}$$

$$u\frac{\partial T}{\partial x} + v\frac{\partial T}{\partial y} = \alpha_{\mathrm{nf}}\left[\frac{\partial^2 T}{\partial x^2} + \frac{\partial^2 T}{\partial y^2}\right] \tag{4}$$

where

$$\alpha_{\mathrm{nf}} = \frac{k_{\mathrm{nf}}}{(\rho Cp)_{\mathrm{nf},0}} \tag{5}$$

where the relationships between the shear stress and shear rate in case of two-dimensional motion in rectangular co-ordinate according to the Ostwald–de Waele model are as follows: [40]

$$\tau = -m\left[\left|\sqrt{\frac{1}{2}(\dot\gamma\cdot\dot\gamma)}\right|^{(n-1)}\right]\dot\gamma \tag{6}$$

where

$$\frac{1}{2}(\dot\gamma\cdot\dot\gamma) = 2\left\{\left(\frac{\partial u}{\partial x}\right)^2 + \left(\frac{\partial v}{\partial y}\right)^2\right\} + \left(\frac{\partial v}{\partial x} + \frac{\partial u}{\partial y}\right)^2 \tag{7}$$

Thus the stress tensors of Eqs. (2) and (3) take the following forms

Table 1
Values of fluid behaviour index parameters (m, n)

Solid volume fraction (ϕ) (%)	m (N sec^n m^{-2})	n
0.5	0.00187	0.880
1.0	0.00230	0.830
1.5	0.00283	0.780
2.0	0.00347	0.730
2.5	0.00426	0.680
3.0	0.00535	0.625
3.5	0.00641	0.580
4.0	0.00750	0.540
4.5	0.00876	0.500
5.0	0.01020	0.460

$$\tau_{xx} = -2\left\{m\left|\left[2\left\{\left(\frac{\partial u}{\partial x}\right)^2 + \left(\frac{\partial v}{\partial y}\right)^2\right\} + \left(\frac{\partial v}{\partial x} + \frac{\partial u}{\partial y}\right)^2\right]^{\frac{1}{2}}\right|^{(n-1)}\right\}\left(\frac{\partial u}{\partial x}\right) \tag{8}$$

$$\tau_{yx} = \tau_{xy} = -\left\{m\left|\left[2\left\{\left(\frac{\partial u}{\partial x}\right)^2 + \left(\frac{\partial v}{\partial y}\right)^2\right\} + \left(\frac{\partial v}{\partial x} + \frac{\partial u}{\partial y}\right)^2\right]^{\frac{1}{2}}\right|^{(n-1)}\right\}\left(\frac{\partial u}{\partial y} + \frac{\partial v}{\partial x}\right) \tag{9}$$

$$\tau_{yy} = -2\left\{m\left|\left[2\left\{\left(\frac{\partial u}{\partial x}\right)^2 + \left(\frac{\partial v}{\partial y}\right)^2\right\} + \left(\frac{\partial v}{\partial x} + \frac{\partial u}{\partial y}\right)^2\right]^{\frac{1}{2}}\right|^{(n-1)}\right\}\left(\frac{\partial v}{\partial y}\right) \tag{10}$$

Here m and n are two empirical constants, which depends on the type of nanofluid used. Putra et al. [34] have shown experimentally the relation between the shear stress and shear strain for Al_2O_3–water nanofluid. Using this data, the values of m and n has been calculated for 1% and 4% solid volume fraction. These values are suitably interpolated and extrapolated keeping in mind that the shear stress decreases with increase in ϕ for a particular shear rate in the mixture. The values of m and n for different ϕ has been given in Table 1. It is to be noted that for a shear thinning fluid the value of n is less than 1 [40]. Since the rate of change of shear stress with shear rate for Cu–water nanofluid is not available, these data of Al_2O_3–water nanofluid has been adopted for Cu–water nanofluid to observe the nature of the heat transfer.

The effective density of the nanofluid at reference temperature is

$$\rho_{\mathrm{nf},0} = (1-\phi)\rho_{f,0} + \phi\rho_{s,0} \tag{11}$$

and the heat capacitance of nanofluid is

$$(\rho Cp)_{\mathrm{nf}} = (1-\phi)(\rho Cp)_f + \phi(\rho Cp)_s \tag{12}$$

as given by Xuan et al. [6].

The effective thermal conductivity of fluid has been determined by the model proposed by Patel et al. [20]. For the two-component entity of spherical-particle suspension the model gives

$$\frac{k_{\mathrm{eff}}}{k_f} = 1 + \frac{k_p A_p}{k_f A_f} + c k_p Pe\frac{A_p}{k_f A_f} \tag{13}$$

where

$$\frac{A_p}{A_f} = \frac{d_f}{d_p}\frac{\phi}{(1-\phi)} \tag{14}$$

and $Pe = \frac{u_p d_p}{\alpha_f}$, where u_p is the Brownian motion velocity of the particles which is given by $u_p = \frac{2k_b T}{\pi \mu_f d_p^2}$.

The calculation of effective thermal conductivity can be obtained from Eq. (13).

The above equations can be converted to non-dimensional form, using the following dimensionless parameters

$$X = x/h, \qquad Y = y/h, \qquad U = uh/\alpha, \qquad V = vh/\alpha$$
$$P = (p - p_0)\cdot h^2/(\rho_{\mathrm{nf},0}\cdot \alpha^2) \quad \text{and}$$
$$\theta = (T - T_C)/(T_H - T_C)$$

Then the non-dimensional equations will be as follows

$$\frac{\partial U}{\partial X} + \frac{\partial V}{\partial Y} = 0 \tag{15}$$

$$U\frac{\partial U}{\partial X} + V\frac{\partial U}{\partial Y} = -\frac{\partial P}{\partial X} + \frac{\mu_{\mathrm{app}}}{\rho_{\mathrm{nf},0}}\frac{}{\alpha_{f,0}}\left[\frac{\partial^2 U}{\partial X^2} + \frac{\partial^2 U}{\partial Y^2}\right] \tag{16}$$

$$U\frac{\partial V}{\partial X} + V\frac{\partial V}{\partial Y} = -\frac{\partial P}{\partial Y} + GrPrPr\frac{\rho_{f,0}}{\rho_{\mathrm{nf},0}}\left(1 - \phi + \phi\frac{\rho_s\beta_s}{\rho_f\beta_f}\right)\theta + \frac{\mu_{\mathrm{app}}}{\rho_{\mathrm{nf},0}}\frac{}{\alpha_{f,0}}\left[\frac{\partial^2 V}{\partial X^2} + \frac{\partial^2 V}{\partial Y^2}\right] \tag{17}$$

$$U\frac{\partial \theta}{\partial X} + V\frac{\partial \theta}{\partial Y} = \frac{k_{\mathrm{nf}}}{k_f}\frac{(\rho Cp)_{f,0}}{(\rho Cp)_{\mathrm{nf},0}}\left[\frac{\partial^2 \theta}{\partial X^2} + \frac{\partial^2 \theta}{\partial Y^2}\right] \tag{18}$$

Here the apparent viscosity of the nanofluid is

$$\mu_{\mathrm{app}} = m\left(\frac{\alpha_{f,0}}{h^2}\right)^{(n-1)}\left|\left[2\left\{\left(\frac{\partial U}{\partial X}\right)^2 + \left(\frac{\partial V}{\partial Y}\right)^2\right\} + \left(\frac{\partial V}{\partial X} + \frac{\partial U}{\partial Y}\right)^2\right]^{\frac{1}{2}}\right|^{(n-1)} \tag{19}$$

The boundary conditions, used to solve Eqs. (15) to (18) are as follows.

$$u = v = \frac{\partial T}{\partial y} = 0 \quad \text{at } y = 0, h \text{ and } 0 \leqslant x \leqslant l$$

i.e.,

$$U = V = \frac{\partial \theta}{\partial Y} = 0 \quad \text{at } Y = 0, 1.0 \text{ and } 0 \leqslant X \leqslant 1.0$$
$$T = T_H, \quad u = v = 0 \quad \text{at } x = 0 \text{ and } 0 \leqslant y \leqslant h$$

i.e.,

$$\theta = 1.0 \quad \text{and} \quad U = V = 0 \quad \text{at } X = 0 \text{ and } 0 \leqslant Y \leqslant 1.0$$
$$T = T_C, \quad u = v = 0 \quad \text{at } x = l \text{ and } 0 \leqslant y \leqslant h$$

i.e.,

$$\theta = 0 \quad \text{and} \quad U = V = 0 \quad \text{at } X = 1.0 \text{ and } 0 \leqslant Y \leqslant 1.0$$

Eqs. (15) to (18), along with the boundary conditions are solved numerically. From the converged solutions, we have calculated Nu_y (local Nusselt number) and $\overline{Nu}$ (average Nusselt number) for the hot wall as follows

Table 2
Comparison of results for validation

Rayleigh number (Ra)	$\overline{Nu}$ of de Vahl Davis [42]	$\overline{Nu}$ of present code
10^4	2.243	2.245
10^5	4.519	4.521
10^6	8.799	8.813

$$Nu_y = -\frac{k_{\mathrm{eff}}}{k_f}\frac{\partial \theta}{\partial X}\bigg|_{X=0,Y} \tag{20}$$

$$\overline{Nu} = \frac{1}{H}\int_0^H Nu_y \cdot \mathrm{d}Y|_{X=0} \tag{21}$$

where, H is dimensionless cavity height.

The dimensionless stream function ψ has been defined as $U = \partial\psi/\partial Y$ and $V = -\partial\psi/\partial X$. The stream function at any grid location (X, Y) is calculated as

$$\psi(X, Y) = \int_{Y0}^{Y} U \cdot \partial Y \psi(X, Y_0) \tag{22}$$

Along the solid boundary the stream function is taken as zero. $\psi(X, Y_0)$ is known either from the previous calculation, or, from the boundary condition.

2.3. Numerical approach and validation

The governing mass, momentum and energy equations has been discretized by a control volume approach using a power law profile approximation. The computational domain has been divided into 81×81 non-uniform grids. Finer grids have been taken at the boundaries. The set of discretized equations have been solved iteratively, through alternate direction implicit ADI, using the SIMPLER algorithm [41]. For convergence, under-relaxation technique has been employed. To check the convergence, the mass residue of each control volume has been calculated and the maximum value has been used to check the convergence. The convergence criterion has been set to 10^{-7}.

The results are validated with the results of de Vahl Davis [42] for different Ra, which has been summarized in Table 2. The difference between the average Nusselt number of de Vahl Davis and that obtained by the present code is well within acceptable limit.

3. Results and discussion

The flow and heat transfer for a range of Ra and ϕ have been studied. Water has been considered as the base fluid with $Pr = 7.02$ (considering base temperature as 20 °C) [43], for our present study. Solid spherical copper nanoparticles of 100 nm diameter mixed with water, has been considered as nanofluid. The effective thermal conductivity of nanofluid has been calculated using the correlation given in [20] for each control volume as the k_{eff} is temperature dependent. The constant 'c' which appears in the correlation has been calculated from the experimental data available for copper water nanofluid [3]. The

Table 3
Thermophysical properties of different phase at 20 °C

Property	Fluid (water)	Solid (copper)
C_p (J/kg K)	4181.80	383.1
ρ (kg/m^3)	1000.52	8954.0
k (W/m K)	0.597	386.0
β (k^{-1})	210.0×10^{-6}	51.0×10^{-6}

average value of constant has been considered for our simulation, which came out as 3.60×10^4 that is in line with result given in Ref. [20]. The physical and thermal properties of both the solid and the fluid at the base temperature i.e. at 20 °C have been summarized in Table 3 [43,44]. The constants m and n for calculating shear stresses have been taken from the experimental observation [34]. Results are presented for $Ra = 10^4$ to 10^7, while ϕ has been varied from 0.0% to 5.0% with the increment of 0.5%. The hot wall temperature has been considered as 303 K (30 °C) while the cold wall temperature is 293 K (20 °C).

Since, the heat transfer is strongly affected by the nature of flow, the flow structure has been considered before discussing the variation of Nusselt number with different parameters.

3.1. Effect of solid volume fraction on vertical velocity and temperature

The vertical velocities (V) at $Y = 0.5$ for $1.0 \geqslant X \geqslant 0.0$, for $Ra = 10^6$ has been presented in Fig. 2, which shows that with the increase in ϕ, the value of maximum velocity decreases. It seems that, as ϕ increases, the density and the viscosity of the nanofluid increases. Though k_{eff} increases with ϕ, the rate of increase of viscosity with ϕ is much higher than that of k_{eff}. As a result the effect of buoyancy decreases, and hence the vertical velocity decreases with increase in ϕ. The velocity boundary layer also getting thicker and the size of the stagnant zone at the core of cavity decreases. This zone is larger for $\phi = 0.0\%$ and smaller for $\phi = 5.0\%$.

Fig. 3 shows the variation of temperature along the mid-plane of the cavity for $Ra = 10^6$. This shows that at $\phi = 0.0\%$ a uniform temperature prevails at the core of cavity because there is no flow. With the increase in ϕ, this zone decreases considerably. As viscosity and k_{eff} both increases with ϕ, the heat penetrates much deeper into the nanofluid, before being carried away by the convection. And hence the thermal boundary layer increases with ϕ.

3.2. Effect of solid volume fraction on streamlines and isotherms

The streamlines and isotherms for $Ra = 10^6$ for $\phi = 0\%$, 2.5%, and 5.0% has been presented in Fig. 4. The figures show that for a particular Ra, the strength of circulation decreases with increase in ϕ. This is due to the decrease in vertical velocity with increase in ϕ. The figures show that the thickness of the velocity boundary layer increases with ϕ as was revealed from Fig. 2. The same pattern can be observed for other Rayleigh numbers. From the isotherms it has been observed that the thermal boundary layer gets thicker due two increase of diffusive heat transfer with increase in ϕ. It is also revealed from Fig. 3. This increment is much more as viscosity increases rapidly with ϕ resulting decrease in buoyancy. For other Rayleigh numbers also the same patterns are observed.

Streamlines and isotherms for $\phi = 2.5\%$ for $Ra = 10^4$, 10^5, and 10^7 has been presented in Fig. 5. Comparing the Figs. 5 and 4(b), it is observed that the strength of circulation increases rapidly with increase in Ra. This is obviously due to increase in buoyancy, as viscosity and density remains same for a particular ϕ. Also the thickness of velocity boundary layer near

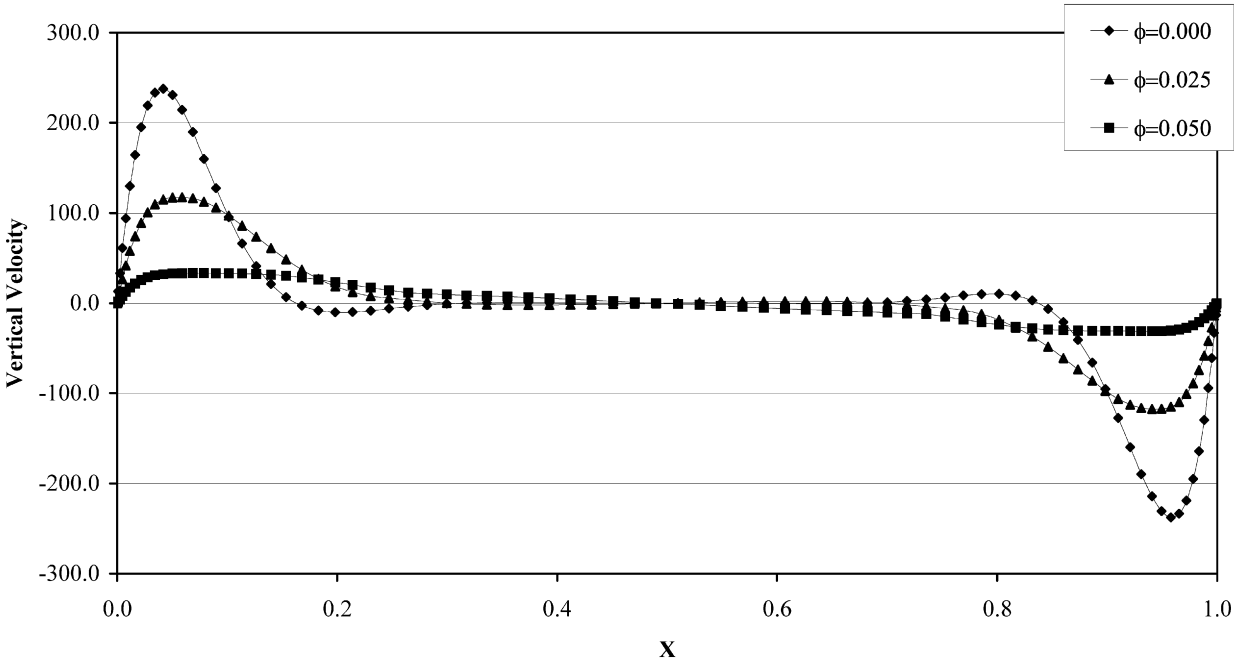

Fig. 2. Vertical velocity profile at mid plane for different ϕ values for $Ra = 10^6$.

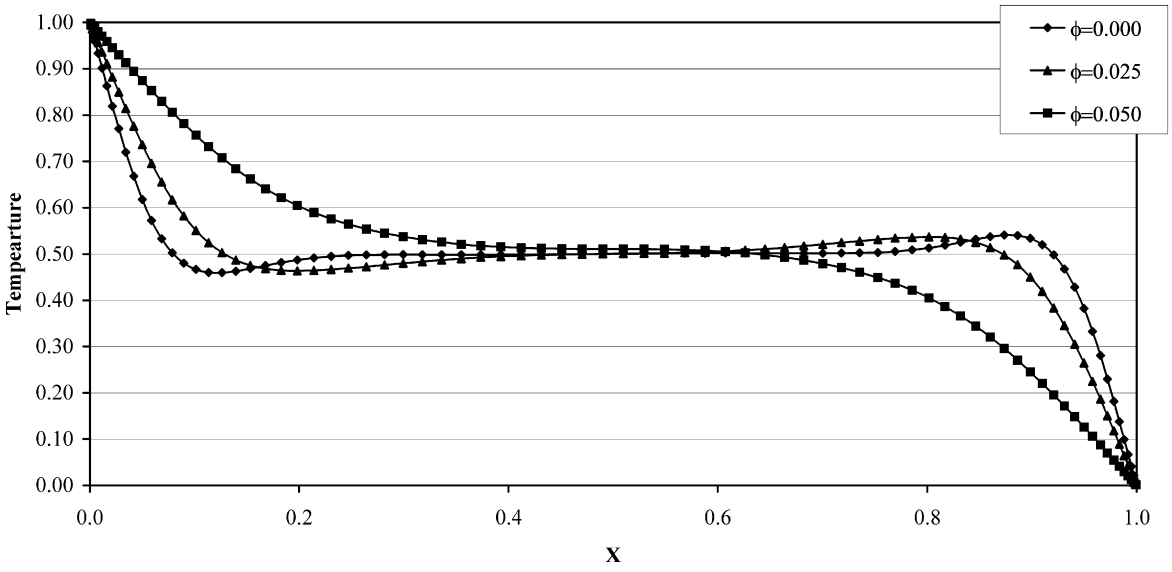

Fig. 3. Temperature profile at mid plane for different ϕ values for $Ra = 10^6$.

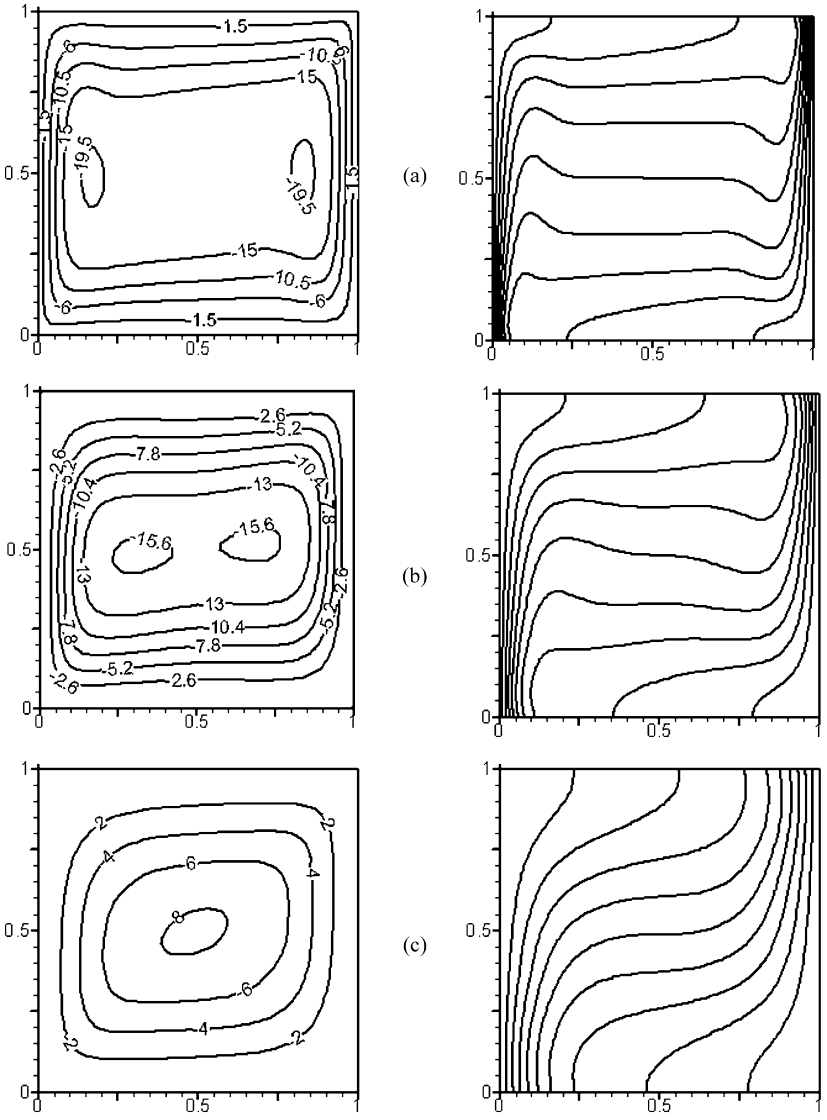

Fig. 4. Streamlines and isotherms for $Ra = 10^6$ and for (a) $\phi = 0.0\%$, (b) $\phi = 2.5\%$, and (c) $\phi = 5.0\%$.

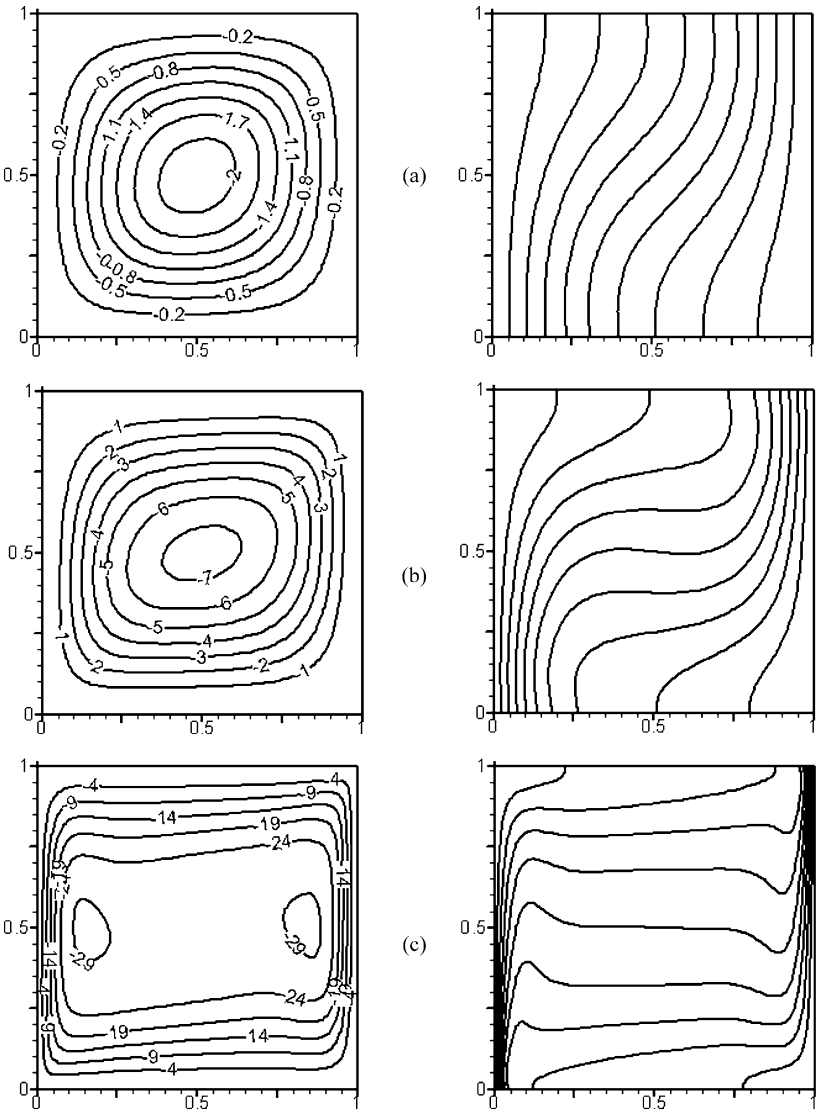

Fig. 5. Streamlines and isotherms for $\phi = 2.5\%$ and for (a) $Ra = 10^4$, (b) $Ra = 10^5$ and (c) $Ra = 10^7$.

the walls decreases and hence the stagnant core zone increases with increase in *Ra*. The thickness of thermal boundary layer near the wall also decreases with increase in *Ra*. The same pattern is observed for other ϕ values also.

3.3. Effect of solid volume fraction on average Nusselt number

The average Nusselt number ($\overline{Nu}$) along the hot wall has been presented for different *Ra* and ϕ (Fig. 6). It shows a steady decrease in $\overline{Nu}$ for increase in ϕ for same *Ra*. Also $\overline{Nu}$ increases with *Ra* for a particular ϕ. The trend is similar to that observed from the experiments of Putra et al. [34] and Wen and Ding [35], where they have found that heat transfer decrease with increase in ϕ. Putra et al. [34] found it with Al_2O_3–water nanofluid as well as CuO–water nanofluid while Wen and Ding [35] found it for TiO_2–water nanofluid. This kind of result may be due to the combined effect of viscosity and thermal conductivity of the nanofluid. As viscosity increases rapidly with increase in ϕ, particularly at low shear rate the effect of buoyancy decreases, which decrease the convective heat transfer rapidly and the increase in thermal conductivity is insufficient to recover the loss. Wen and Ding [35] has also expressed similar kind of view. It has also been observed that at low *Ra* i.e. at 10^4 and 5×10^4, heat transfer becomes stagnant at higher ϕ (above 3%). Most probably in this case the decrease in convective heat transfer is compensated by increase in conductive heat transfer.

4. Conclusion

Heat transfer enhancement using copper–water nanofluid in a two dimensional enclosure has been studied numerically for a range of Rayleigh number 10^4 to 10^7, with a wide range of solid volume fraction ($5.0\% \geqslant \phi \geqslant 0.0$). The diameter of copper particle is 100 nm and Prandtl number of clear fluid is 7.02. The numerical analysis has been performed using primitive variables. The fluid has been considered as non-Newtonian in nature. The Ostwald–de Waele model for a non-Newtonian shear thinning fluid has been considered to calculate shear stresses. The constants for model have been taken from the experiment

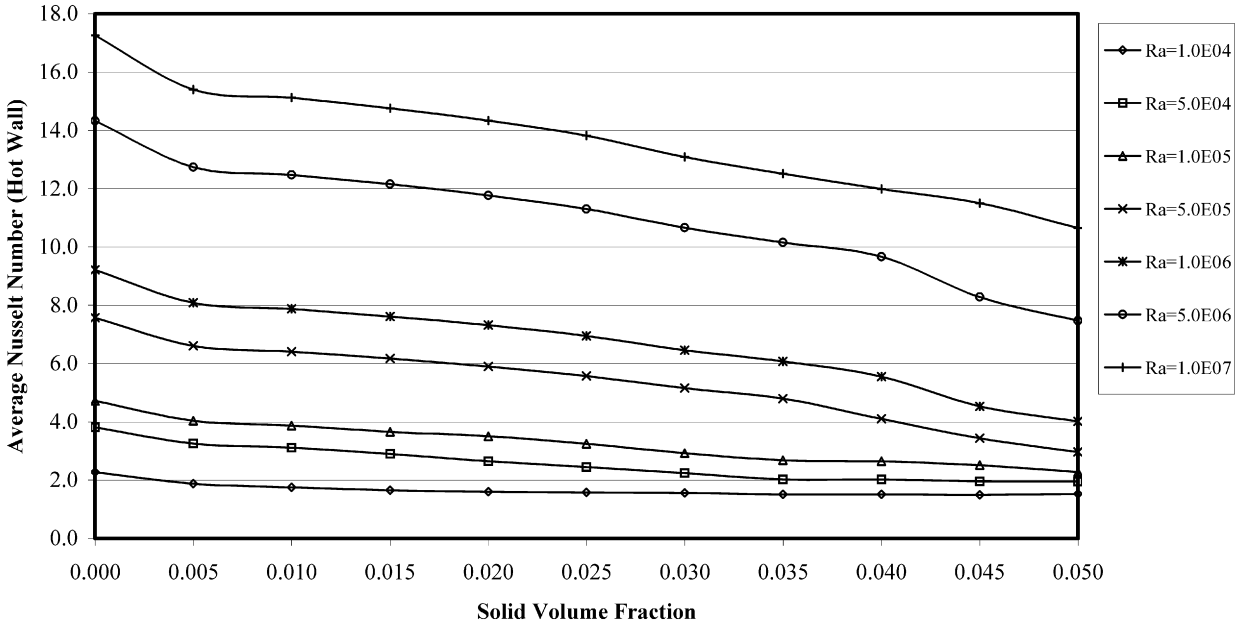

Fig. 6. Variation of average Nusselt number with solid volume fraction for different *Ra*.

of Putra et al. [34]. The effective thermal conductivity of the nanofluids has been predicted using the model proposed by Patel et al. [20]. The results show a considerable decrease in heat transfer for increase in solid volume fraction for any Rayleigh number. However at low *Ra*, the heat transfer remains almost constant when ϕ exceeds 3%. For $\phi = 5.0\%$ the decrease in average Nusselt number is about 32.8% compared to clear fluid when $Ra = 10^4$ and about 38.3% when $Ra = 10^7$. Heat transfer increases with increase in Rayleigh number for a particular ϕ. Experiments needs to be carried out to find the actual values of m and n for this kind of nanofluid and actual heat transfer in this kind of geometrical configuration.

References

[1] S. Lee, S.U.S. Choi, S. Li, J.A. Eastman, Measuring thermal conductivity of fluids containing oxide nanoparticles, Trans. ASME J. Heat Transfer 121 (1999) 280–289.

[2] J.A. Eastman, S.U.S. Choi, S. Li, W. Yu, L.J. Thompson, Anomalously increased effective thermal conductivities of ethylene glycol-based nanofluids containing copper nanoparticles, Appl. Phys. Lett. 78 (2001) 718–720.

[3] Y. Xuan, Q. Li, Heat transfer enhancement of nanofluids, Int. J. Heat Fluid Flow 21 (2000) 58–64.

[4] H.E. Patel, S.K. Das, T. Sundarrajan, A.S. Nair, B. George, T. Pradeep, Thermal conductivities of naked and monolayer protected metal nanoparticle based nanofluids: Manifestation of anomalous enhancement and chemical effects, Appl. Phys. Lett. 83 (2003) 2931–2933.

[5] D.W. Zhou, Heat transfer enhancement of copper nanofluid with acoustic cavitation, Int. J. Heat Mass Transfer 47 (2004) 3109–3117.

[6] Y. Xuan, W. Roetzel, Conceptions for heat transfer correlation of nanofluids, Int. J. Heat Mass Transfer 43 (2000) 3701–3707.

[7] P. Keblinski, S.R. Phillpot, S.U.S. Choi, J.A. Eastman, Mechanisms of heat flow in suspensions of nano-sized particles (nanofluids), Int. J. Heat Mass Transfer 45 (2002) 855–863.

[8] L. Xue, P. Keblinski, S.R. Phillpot, S.U.S. Choi, J.A. Eastman, Effect of liquid layering at the liquid–solid interface on thermal transport, Int. J. Heat Mass Transfer 47 (2004) 4277–4284.

[9] S.K. Das, N. Putra, P. Thiesen, W. Roetzel, Temperature dependence of thermal conductivity enhancement for nanofluids, J. Heat Transfer 125 (2003) 567–574.

[10] R.L. Hamilton, O.K. Crosser, Thermal conductivity of heterogeneous two-component systems, I & EC Fundamentals 1 (1962) 182–191.

[11] F.J. Wasp, Solid–Liquid Flow Slurry Pipeline Transportation, Trans. Tech. Publ., Berlin, 1977.

[12] J.C. Maxwell-Garnett, Colours in metal glasses and in metallic films, Philos. Trans. Roy. Soc. A 203 (1904) 385–420.

[13] D.A.G. Bruggeman, Berechnung Verschiedener Physikalischer Konstanten von Heterogenen Substanzen, I. Dielektrizitatskonstanten und Leitfahigkeiten der Mischkorper aus Isotropen Substanzen, Annalen der Physik. Leipzig 24 (1935) 636–679.

[14] B.X. Wang, L.P. Zhou, X.F. Peng, A fractal model for predicting the effective thermal conductivity of liquid with suspension of nanoparticles, Int. J. Heat Mass Transfer 46 (2003) 2665–2672.

[15] W. Yu, S.U.S. Choi, The role of interfacial layer in the enhanced thermal conductivity of nanofluids: A renovated Maxwell model, J. Nanoparticles Res. 5 (2003) 167–171.

[16] D.H. Kumar, H.E. Patel, V.R.R. Kumar, T. Sundararajan, T. Pradeep, S.K. Das, Model for conduction in nanofluids, Phys. Rev. Lett. 93 (2004) 144301-1-3.

[17] R. Prasher, P. Bhattacharya, P.E. Phelan, Brownian-motion-based convective–conductive model for the effective thermal conductivity of nanofluid, ASME J. Heat Transfer 128 (2006) 588–595.

[18] Das, et al., Reply, Phys. Rev. Lett. 95 (2005) 019402.

[19] Das, et al., Reply, Phys. Rev. Lett. 95 (2005) 209402.

[20] H.E. Patel, T. Sundarrajan, T. Pradeep, A. Dasgupta, N. Dasgupta, S.K. Das, A micro-convection model for thermal conductivity of nanofluid, Pramana J. Phys. 65 (2005) 863–869.

[21] Y. Xuan, Q. Li, Investigation on convective heat transfer and flow features of nanofluids, J. Heat Transfer 125 (2003) 151–155.

[22] Y. Yang, Z.G. Zhang, A.R. Grukle, W.B. Anderson, G. Wu, Heat transfer properties of nanoparticle-in-fluid dispersions (nanofluids) in laminar flow, Int. J. Heat Mass Transfer 48 (2005) 1107–1116.

[23] J. Buongiorno, Convective transport in nanofluids, J. Heat Transfer 128 (2006) 240–250.

[24] J. Koo, C. Kleinstreuer, Impact analysis of nanoparticle motion mechanisms on the thermal conductivity of nanofluids, Int. Commun. Heat Mass Transfer 32 (2005) 1111–1118.

[25] S.Z. Heris, M.N. Esfahany, S.Gh. Etemad, Experimental investigation of convective heat transfer of Al_2O_3/water nanofluid in circular tube, Int. J. Heat Fluid Flow 28 (2007) 203–210.
[26] S.Z. Heris, S.Gh. Etemad, M.N. Esfahany, Experimental investigation of oxide nanofluids laminar flow convective heat transfer, Int. Comm. Heat Mass Transfer 33 (2006) 529–535.
[27] H.C. Brinkman, The viscosity of concentrated suspensions and solutions, J. Chem. Phys. 20 (1952) 571–581.
[28] K. Kwak, C. Kim, Viscosity and thermal conductivity of copper oxide nanofluid dispersed in ethylene glycol, Korea–Australia Rheology J. 17 (2005) 35–40.
[29] H. Chang, C.S. Jwo, C.H. Lo, T.T. Tsung, M.J. Kao, H.M. Lin, Rheology of CuO nanoparticle suspension prepared by ASNSS, Rev. Adv. Mater. Sci. 10 (2005) 128–132.
[30] Y. Ding, H. Alias, D. Wen, R.A. Williams, Heat transfer of aqueous suspensions of carbon nanotubes (CNT nanofluids), Int. J. Heat Mass Transfer 49 (2006) 240–250.
[31] S.E.B. Maiga, C.T. Nguyen, N. Galanis, G. Roy, Heat transfer behaviours of nanofluids in a uniformly heated tube, Superlattices and Microstructures 35 (2004) 543–557.
[32] M. Okada, T. Suzuki, Natural convection of water-fine particle suspension in a rectangular cell, Int. J. Heat Mass Transfer 40 (1997) 3201–3208.
[33] C. Kang, M. Okada, A. Hattori, K. Oyama, Natural convection of water-fine particle suspension in a rectangular vessel heated and cooled from opposing vertical walls (classification of the natural convection in the case of suspension with narrow-size distribution), Int. J. Heat Mass Transfer 44 (2001) 2973–2982.
[34] N. Putra, W. Roetzel, S.K. Das, Natural convection of nano-fluids, Heat Mass Transfer 39 (2003) 775–784.
[35] D. Wen, Y. Ding, Natural convective heat transfer of suspensions of titanium dioxide nanoparticles (nanofluids), IEEE Trans. Nanotechnol. 5 (2006) 220–227.
[36] K. Khanafer, K. Vafai, M. Lightstone, Buoyancy-driven heat transfer enhancement in a two-dimensional enclosure utilizing nanofluids, Int. J. Heat Mass Transfer 46 (2003) 3639–3653.
[37] R.Y. Jou, S.C. Tzeng, Numerical research of nature convective heat transfer enhancement filled with nanofluids in rectangular enclosures, Int. Commun. Heat Mass Transfer 33 (2006) 727–736.
[38] A.K. Santra, S. Sen, N. Chakraborty, Comparison of heat transfer augmentation in a square cavity using nanofluid following two different thermal conductivity models, J. Energy Heat Mass Transfer 29 (2007) 289–310.
[39] P.K. Mandal, S. Chakravarty, A. Mandal, N. Amin, Effect of body acceleration on unsteady pulsatile flow of non-Newtonian fluid through a stenosed artery, Appl. Math. Comput. 189 (2007) 766–779.
[40] R.B. Bird, W.E. Stewert, E.N. Lightfoot, Transport Phenomena, John Wiley & Sons, Singapore, 1960.
[41] S.V. Patankar, Numerical Heat Transfer and Fluid Flow, Hemisphere, Washington, DC, 1980.
[42] G. de Vahl Davis, Natural convection of air in a square cavity, a benchmark numerical solution, Int. J. Numer. Methods Fluids 3 (1962) 249–264.
[43] M.N. Ozisik, Heat Transfer—A Basic Approach, McGraw–Hill, 1985.
[44] Website of Western Washington University, Bellingham, Washington, http://www.ac.wwu.edu/~vawter/PhysicsNet/Topics/Thermal/ThermExpan.htm.